CDS

TECHNICAL MEMORANDUM NO. CIT-CDS 96-013
August, 1996

"Mechanical Integrators Derived from a Discrete Variational Principle"

Jeffrey M. Wendlandt and Jerrold E. Marsden

Control and Dynamical Systems
California Institute of Technology

Mechanical Integrators Derived from a Discrete Variational Principle

Jeffrey M. Wendlandt*
Mechanical Engineering
University of California at Berkeley
wents@eecs.berkeley.edu
http://robotics.eecs.berkeley.edu/~wents/

Jerrold E. Marsden†
Control and Dynamical Systems
California Institute of Technology
104-44 Pasadena CA 91125
marsden@cds.caltech.edu
http://cds.caltech.edu/~marsden/

August 23, 1996

Abstract

Many numerical integrators for mechanical system simulation are created by using discrete algorithms to approximate the continuous equations of motion. In this paper, we present a procedure to construct time-stepping algorithms that approximate the flow of continuous ODE's for mechanical systems by discretizing Hamilton's principle rather than the equations of motion. The discrete equations share similarities to the continuous equations by preserving invariants, including the symplectic form and the momentum map. We first present a formulation of discrete mechanics along with a discrete variational principle. We then show that the resulting equations of motion preserve the symplectic form and that this formulation of mechanics leads to conservation laws from a discrete version of Noether's theorem. We then use the discrete mechanics formulation to develop a procedure for constructing mechanical integrators for continuous Lagrangian systems. We apply the construction procedure to the rigid body and the double spherical pendulum to demonstrate numerical properties of the integrators.

Contents

*Ph.D. candidate; Research partially supported by DOE contract DE-FG03-95ER-25251.
†Research partially supported by DOE contract DE-FG03-95ER-25251 and the California Institute of Technology.

List of Figures

List of Tables

1 Introduction

Goals. The goal of this paper is to present a systematic construction of mechanical integrators for simulating finite dimensional mechanical systems with symmetry based on a discretization of Hamilton's principle. We strive for a method that is theoretically attractive and numerically competitive. Of course, we do not claim that the methods will be superior in very specific problems for which custom methods may be available (as, for example, in symplectic integrators for the solar system—see, for example, (Wisdom and Holman, 1991)).

Mechanical Integrators. These are numerical integration methods that preserve some of the invariants of the mechanical system, such as, energy, momentum, or the symplectic form. It is well known that if the energy and momentum map include all the integrals from a certain class (depending on the smoothness available) that one cannot create integrators that are symplectic, energy preserving, *and* momentum preserving unless they coincidentally integrate the equations exactly up to a time parametrization (see (Ge and Marsden, 1988) for the exact statement). Thus, mechanical integrators divide into two overall classes, *symplectic-momentum* and *energy-momentum* integrators. It is the hope that by exploiting the structure of mechanical systems, one can create mechanical integrators that are not only theoretically attractive, but are more computationally efficient and have better long term simulation properties than conventional integration schemes. The overall situation for mechanical integrators is of course a complex one, and it is still evolving. We refer to (Marsden and G. Patrick, 1996) for a recent collection of papers in the area and for additional references and to (Marsden, 1992) for some additional background.

The Main Technique of This Paper. This paper presents a method to construct symplectic-momentum integrators for Lagrangian systems defined on a linear space with holonomic constraints. The constraint manifold, Q, is regarded as embedded in the linear space, V. A discrete version of the Lagrangian is then formed and a discrete variational principle is applied to the discrete Lagrangian system. The resulting discrete equations define an implicit (explicit in some cases) numerical integration algorithm on $Q \times Q$ that approximates the flow of the continuous Euler-Lagrange equations on TQ. The algorithm equations are called the *discrete Euler-Lagrange (DEL)* equations.

The DEL equations share similarities to the continuous Euler-Lagrange equations. The DEL equations preserve a symplectic form defined in the paper and preserve a discrete momentum derived through a discrete Noether's theorem. The discrete momentum corresponding to invariance of the continuous Lagrangian system to a linear group action is conserved, and the value of the discrete momentum approaches the value of the continuous momentum as the step size decreases. In general, the method does not preserve energy for conservative Lagrangian systems, but the numerical examples suggest that the energy varies about a constant value. The energy variations decrease and the constant value approaches the continuous energy as the step size decreases.

We treat holonomic constraints through constraint functions on the linear space. The constraints are satisfied at each time step through the use of Lagrange multipliers.

The Examples Considered. The construction procedure is applied to two examples and numerical results are presented.

1. **The Rigid Body**. The method is applied to the rigid body to produce evolution equations in terms of unit quaternions. We take the linear space, V, to be $\mathbb{R}^4$, and the constraint manifold, $Q \subset V$, to be S^3.

2. **The Double Spherical Pendulum.** The method is also applied to the double spherical pendulum. The linear space, V, is $\mathbb{R}^3 \times \mathbb{R}^3$, and the constraint manifold, $Q \subset V$, is $S^2 \times S^2$. We compare the integrator to an energy-momentum integrator.

For both examples, the momentum, energy, accuracy, and efficiency is examined. The examples suggest that accurate results are achieved with large step sizes.

Some of the Literature. This paper uses the discrete variational principle presented in (Veselov, 1988) and again in (Veselov, 1991) and (Moser and Veselov, 1991). It is shown in (Veselov, 1988) that the DEL equations preserve a symplectic form. The same discrete mechanics procedure is derived in (Baez and Gilliam, 1995) using an algebraic approach, and they also show that there is a discrete Noether's theorem for infinitesimal symmetry.

Various authors have proposed versions of discrete mechanics. Some study discrete mechanics without the motivation of constructing integration schemes while this is a definite motivation for other authors. In (Maeda, 1981), the author presents a version of discrete mechanics based on the concept of a difference space. The author later shows how to derive the discrete equations from a discrete version of Hamilton's variational principle, the same discretization later used in (Veselov, 1988). (Maeda, 1981) also presents a version of Noether's theorem. A different approach to discrete mechanics for point mass systems not derived from a variational principle is shown in (Labudde and Greenspan, 1974), (Labudde and Greenspan, 1976a), and (Labudde and Greenspan, 1976b). These algorithms preserve energy and momentum. Another discussion of discretizing variational principles is given in (MacKay, 1992) and in (Lewis and Kostelec, 1996). It is our opinion that the approach in (Veselov, 1988) we adopt in this paper is the most appealing theoretically of these methods and, in addition, is numerically competitive.

Some authors discretize the principle of least action instead of Hamilton's principle. Algorithms that conserve the Hamiltonian are derived in (Itoh and Abe, 1988) based on difference quotients. Differentiation is not used and the action is extremized using variational difference quotients. This development presents multistep methods with variable time steps. The least action principle is discretized in a different way

in (Shibberu, 1994). The resulting equations explicitly enforce energy, and it is stated that the equations preserve quadratic invariants.

Various energy-momentum integrators have been developed by Simo and his co-workers. See, for example, (Simo and Tarnow, 1992). Recently, energy-momentum integrators have been derived based on discrete directional derivatives and discrete versions of Hamiltonian mechanics in (Gonzalez, 1996a). More references on energy-momentum methods are in the reference section of (Gonzalez, 1996a) and in (Gonzalez, 1996b). Symplectic, momentum and energy conserving schemes for the rigid body are presented in (Lewis and Simo, 1995).

There is a vast amount of literature on symplectic schemes for Hamiltonian systems. The overview of symplectic integrators in (Sanz-Serna, 1991) provides background and references. See also (Channell and Scovel, 1990) for a survey of the early work and (McLachlan and Scovel, 1996) for a presentation of open problems in symplectic integration. References related to the work in this paper are (Reich, 1993), (Reich, 1994), (McLachlan and Scovel, 1995), and (Jay, 1996). In (Reich, 1993), an integration method is presented for Hamiltonian systems that enforces position and velocity constraints in such a way to make the overall method symplectic. It is shown in (McLachlan and Scovel, 1995) and in (Reich, 1994) that the algorithm also conserves momentum corresponding to a linear symmetry group when the constraint manifold is embedded in a linear space. For another treatment of algorithms formed by embedding the constraint manifold in a linear space, see (Barth and Leimkuhler, 1996b) and (Leimkuhler and Patrick, 1996). The algorithm presented in this paper also embeds the constraint manifold in a linear space but only enforces position constraints.

Comments on Other Algorithms The *Verlet* algorithm (Verlet, 1967) is important in molecular dynamics simulation (Leimkuhler and Skeel, 1994). An extension of the *Verlet* algorithm to handle holonomic constraints is SHAKE (Ryckaert et al., 1977). SHAKE was extended to handle velocity constraints with RATTLE (Anderson, 1983). For a presentation of the symplectic nature of the *Verlet*, SHAKE, and RATTLE algorithms, see (Leimkuhler and Skeel, 1994). The construction method developed in this paper when applied to a Lagrangian with a constant mass matrix and a potential energy term produces an integration method similar to the SHAKE algorithm written in terms of position coordinates. However, the potential force terms differ as can be seen in Equation (4.8). If one applies the construction procedure with the discrete Lagrangian definition in Equation (4.20), then one can reproduce the SHAKE algorithm. One recovers the *Verlet* algorithm if the Lagrangian system has no constraints. This result also appears in (Gillilan and Wilson, 1992), and the discrete variational principle they apply is similar to the principle in (Veselov, 1988). However, they don't extend the result to constraints or more general Lagrangians and do not use the discrete Lagrangian definition in this paper. The emphasis in (Gillilan and Wilson, 1992) is also on calculating a path given end point conditions. Our procedure can handle more general Lagrangians, such as the Lagrangian for the rigid body in terms of quaternions.

Accuracy The construction method produces 2-step methods that have a second order local truncation error. The position error in the numerical examples show second order convergence. One may be able to use the methods in (Yoshida, 1990) to increase the order of accuracy.

The Role of Dissipation. Dissipation is of course very important for practical simulations of mechanical systems. However, our philosophy, which is consistent with that of many other authors (*e.g.*, (Armero and Simo, 1996), (Chorin et al., 1978)) is that of understanding well the ideal model first, and then one can use a time-splitting (product formula) method to interleave it with ones favorite dissipative method one wishes to use.

Energy as a Monitor. In the simulations, we use energy as a monitor to catch any obvious problems, as in (Channell and Scovel, 1990) and (Simo and Gonzalez, 1993). It is still unknown if this is a reliable indicator, but based on the Ge-Marsden result mentioned before, it may well be. Another indication is the analysis with energy oscillation and nearby Hamiltonian systems in (Sanz-Serna, 1991)(page 277–278) and (Sanz-Serna and Calvo, 1994)(page 139–140). We must note, however, that energy conservation alone does

not imply good performance as is shown in (Ortiz, 1986). In our examples, we observe energy oscillations around a constant value, which we take as a good indication.

When comparing energy-momentum and symplectic-momentum methods, it should be kept in mind that energy-momentum methods should be monitored using how well they conserve the symplectic form. This is of course not so straightforward as monitoring using the energy, since the symplectic condition involves computing the derivative of the flow map (*e.g.*, using a cloud of initial conditions). This paper does not directly address these questions, but it is important to keep them in mind.

Outline of the Paper. The paper first presents the discrete variational principle and then derives the properties of the discrete Euler-Lagrange (DEL) equations in a consistent notation. The preserved symplectic form is derived followed by a development of the discrete Noether's theorem. The paper then uses the discrete variational principle (DVP) to develop a construction procedure for mechanical integrators. A construction procedure is presented for constrained and generalized coordinates followed by a discussion of the structure of the Jacobian relevant to solving the DEL equations. It is then shown that the DEL equations have a second order local truncation error, and that the DEL equations have a solution for a small enough time step as long as the continuous Euler-Lagrange equations are solvable. The definition for the discrete momentum is then presented. The method is applied to the rigid body (RB) and the double spherical pendulum (DSP) and numerical results are presented. The paper concludes with a discussion of future work.

2 Discrete Variational Principle

A *discrete variational principle (DVP)* is presented in this section that leads to evolution equations that are analogous to the Euler-Lagrange equations. We call the evolution equations *discrete Euler-Lagrange (DEL)* equations. The results in this section have appeared in (Veselov, 1988), (Veselov, 1991), (Moser and Veselov, 1991) and in (Baez and Gilliam, 1995) but are rederived here in a consistent notation for completeness and clarity.

Given a configuration space, Q, a *discrete Lagrangian* is a map $\mathbb{L} : Q \times Q \to \mathbb{R}$. We will give a procedure that defines the evolution map for the system. The *action sum* is the map $\mathbb{S} : Q^{N+1} \to \mathbb{R}$ defined by

$$\mathbb{S} = \sum_{k=0}^{N-1} \mathbb{L}\left(q_{k+1}, q_k\right), \tag{2.1}$$

where $q_k \in Q$ and $k \in \mathbb{Z}$ is the discrete time. The *discrete variational principle* states that the evolution equations extremize the action sum given fixed end points, q_0 and q_N. Extremizing $\mathbb{S}$ over $q_1, \cdots, q_{N-1}$ leads to the DEL equations:

$$D_2\mathbb{L}\left(q_{k+1}, q_k\right) + D_1\mathbb{L}\left(q_k, q_{k-1}\right) = 0 \quad \text{for all } k \in \{1, \cdots, N-1\} \tag{2.2}$$

or

$$D_2\mathbb{L} \circ \Phi + D_1\mathbb{L} = 0, \tag{2.3}$$

where $\Phi : Q \times Q \to Q \times Q$ is defined implicitly by $\Phi\left(q_k, q_{k-1}\right) = \left(q_{k+1}, q_k\right)$. If $D_2\mathbb{L}$ is invertible, then Equation (2.3) defines the discrete map, Φ, which flows the system forward in discrete time.

3 Invariance Properties

The symplectic structure of $Q \times Q$ is defined in this section and an equation for the symplectic form on $Q \times Q$ is given. It is then shown that Φ preserves the symplectic form. We then derive a discrete Noether's theorem by showing that invariance of the discrete Lagrangian leads to a conserved quantity, a momentum map, for the flow of Φ.

3.1 Symplectic Structure

We first define a fiber derivative by

$$\begin{aligned} \mathbb{FL} : Q \times Q &\rightarrow T^*Q \\ (q_1, q_0) &\mapsto (q_0, D_2\mathbb{L}(q_1, q_0)) \end{aligned} \tag{3.1}$$

and define the 2-form on $Q \times Q$ by pulling back the canonical 2-form on T^*Q:

$$\begin{aligned} \omega &= \mathbb{FL}^*(\Omega_{\text{CAN}}) \\ &= \mathbb{FL}^*(-d\Theta_{\text{CAN}}) \\ &= -d(\mathbb{FL}^*(\Theta_{\text{CAN}})). \end{aligned} \tag{3.2}$$

Choose coordinates, q^i, on Q and choose the canonical coordinates, (q^i, p_i), on T^*Q. In these coordinates, $\Omega_{\text{CAN}} = dq^i \wedge dp_i$ and $\Theta_{\text{CAN}} = p_i dq^i$. The DEL equations are

$$\frac{\partial \mathbb{L}}{\partial q_k^i} \circ \Phi(q_{k+1}, q_k) + \frac{\partial \mathbb{L}}{\partial q_{k+1}^i}(q_{k+1}, q_k) = 0 \tag{3.3}$$

or

$$\frac{\partial \mathbb{L}}{\partial q_{k+1}^i}(q_{k+2}, q_{k+1}) + \frac{\partial \mathbb{L}}{\partial q_{k+1}^i}(q_{k+1}, q_k) = 0. \tag{3.4}$$

Continuing the calculations in Equation (3.2) gives

$$\omega = -d\left(\frac{\partial \mathbb{L}}{\partial q_k^i}(q_{k+1}, q_k)\right) dq_k^i \tag{3.5}$$

$$= -\frac{\partial^2 \mathbb{L}}{\partial q_k^i \partial q_{k+1}^j}(q_{k+1}, q_k)\, dq_{k+1}^j \wedge dq_k^i - \frac{\partial^2 \mathbb{L}}{\partial q_k^i \partial q_k^j}(q_{k+1}, q_k)\, dq_k^j \wedge dq_k^i \tag{3.6}$$

$$= \frac{\partial^2 \mathbb{L}}{\partial q_k^i \partial q_{k+1}^j}(q_{k+1}, q_k)\, dq_k^i \wedge dq_{k+1}^j, \tag{3.7}$$

since the second term in Equation (3.6) vanishes.

3.2 Preservation of the Symplectic Form

We now show that Φ preserves the symplectic form, *i.e.* $\Phi^*\omega = \omega$ where Φ^* is the pullback of Φ. For clarity, let $\Phi(y, x) = (u, v)$ and write $\omega = d(p(y, x)dx) = D_{12}\mathbb{L}(y, x)dx \wedge dy$. In this notation, $y = v = q_{k+1}$, $x = q_k$, and $u = q_{k+2}$. We now show that $\Phi^*\omega = \omega$:

$$\Phi^*\omega = \Phi^*\left(-d\left(\frac{\partial \mathbb{L}}{\partial v^i}(u, v)\, dv^i\right)\right) \tag{3.8}$$

$$= -d\left(\Phi^*\left(\frac{\partial \mathbb{L}}{\partial v^i}(u, v)\, dv^i\right)\right) \tag{3.9}$$

$$= -d\left(\frac{\partial \mathbb{L}}{\partial v^i} \circ \Phi(y, x)\, d\left(v^i(y, x)\right)\right) \tag{3.10}$$

$$= -d\left(-\frac{\partial \mathbb{L}}{\partial y^i}(y, x)\, dy^i\right) \tag{3.11}$$

$$= \frac{\partial^2 \mathbb{L}}{\partial x^j \partial y^i} dx^j \wedge dy^i \tag{3.12}$$

$$= \omega \tag{3.13}$$

We have used Equation (3.4) and the fact that $d(v(y, x)) = dy$ in deriving Equation (3.11) from Equation (3.10).

3.3 Discrete Noether's Theorem

We now derive a discrete version of Noether's theorem. Let the discrete Lagrangian be invariant under the diagonal action of a Lie group G on Q, and let $\xi \in \mathfrak{g}$ where $\mathfrak{g}$ is the Lie algebra of G. Invariance of $\mathbb{L}$ implies that

$$\mathbb{L}(\exp(s\xi)q_{k+1}, \exp(s\xi)q_k) = \mathbb{L}(q_{k+1}, q_k). \tag{3.14}$$

Differentiating Equation (3.14) and setting $s = 0$ implies that

$$D_1\mathbb{L}(q_{k+1}, q_k) \cdot \xi_Q(q_{k+1}) + D_2\mathbb{L}(q_{k+1}, q_k) \cdot \xi_Q(q_k) = 0, \tag{3.15}$$

where ξ_Q is the infinitesimal generator. Consider the action sum, Equation (2.1), where $0 < i < N$ and vary q_{k+1} over $s \in \mathbb{R}$ by $q_{k+1}(s) = \exp(s\xi)\, q_{k+1}$. Since $q_{k+1}(0)$ extremizes $\mathbb{S}$, we have

$$\left.\frac{d\mathbb{S}}{ds}\right|_{s=0} = 0. \tag{3.16}$$

Equation (3.16) implies that

$$D_1\mathbb{L}(q_{k+1}, q_k) \cdot \xi_Q(q_{k+1}) + D_2\mathbb{L}(q_{k+2}, q_{k+1}) \cdot \xi_Q(q_{k+1}) = 0. \tag{3.17}$$

Subtracting Equation (3.15) from Equation (3.17) reveals that

$$D_2\mathbb{L}(q_{k+2}, q_{k+1}) \cdot \xi_Q(q_{k+1}) - D_2\mathbb{L}(q_{k+1}, q_k) \cdot \xi_Q(q_k) = 0. \tag{3.18}$$

If we define the momentum map, $\mathbb{J} : Q \times Q \to \mathfrak{g}^*$, by

$$\langle \mathbb{J}(q_{k+1}, q_k), \xi \rangle \stackrel{\triangle}{=} \langle D_2\mathbb{L}(q_{k+1}, q_k), \xi_Q(q_k) \rangle, \tag{3.19}$$

then Equation (3.18) shows that the momentum map is preserved by $\Phi : Q \times Q \to Q \times Q$.

We note that this $\mathbb{J}$ is equivariant with respect to the action of G on $Q \times Q$ and the coadjoint action of G on $\mathfrak{g}^*$. This is proved as in the case of usual Lagrangians (see (Marsden and Ratiu, 1994)). We also note that one can develop a theory of Lagrangian reduction in the discrete case, as with the continuous case (see (Marsden and Scheurle, 1993)).

4 Construction of Mechanical Integrators

We show in this section how to construct mechanical integrators for continuous Lagrangian systems from the discrete variational principle. We first show how to construct integrators for Lagrangian systems with holonomic constraints by enforcing the constraints through Lagrange multipliers. We call this method the constrained coordinate formulation. We then present a second construction procedure by choosing a set of generalized coordinates. The next section proves that the two methods are equivalent. We then show that the Jacobian used to solve the nonlinear equations for the constrained coordinate formulation has a special structure that can be exploited to increase simulation efficiency. Results are then presented on local truncation error and solvability. We finally relate the discrete-time momentum map and symplectic form to the continuous-time counterparts.

4.1 Constrained Coordinate Formulation

We assume that we have a mechanical system with a constraint manifold, $Q \subset V$, where V is a real, finite dimensional vector space, and that we have an *unconstrained Lagrangian*, $L : TV \to \mathbb{R}$ which, by restriction of L to TQ, defines a *constrained Lagrangian*, $L^c : TQ \to \mathbb{R}$. We also assume that we have a vector valued constraint function, $g : V \to \mathbb{R}^k$, such that $g^{-1}(0) = Q \subset V$ with 0 a regular value of g. The dimension of

V is denoted n, and therefore, the dimension of Q is $m = n - k$. We first define the *discrete, unconstrained Lagrangian*, $\mathbb{L} : V \times V \to \mathbb{R}$, to be

$$\mathbb{L}(y, x) = L\left(\frac{y+x}{2}, \frac{y-x}{h}\right), \tag{4.1}$$

where $h \in \mathbb{R}_+$ is the time step. The *unconstrained action sum* is defined by

$$\mathbb{S} = \sum_{k=0}^{N-1} \mathbb{L}\left(v_{k+1}, v_k\right). \tag{4.2}$$

We then extremize $\mathbb{S} : V^{N+1} \to \mathbb{R}$ subject to the constraint that $v_k \in Q \subset V$ for $k \in \{1, \cdots, N-1\}$,

$$\begin{gathered} \min_{v_k \in V, \lambda_k \in \Lambda} \left(\mathbb{S} + \sum_{k=1}^{N-1} \lambda_k^T g\left(v_k\right)\right) \\ \text{subject to } g(v_k) = 0 \quad \text{for all } k \in \{1, \cdots, N-1\}, \end{gathered} \tag{4.3}$$

to derive that

$$\begin{aligned} D_2\mathbb{L}\left(v_{k+1}, v_k\right) + D_1\mathbb{L}\left(v_k, v_{k-1}\right) + \lambda_k^T Dg\left(v_k\right) = 0 \quad &\text{(no sum over } k\text{)} \\ g\left(v_k\right) = 0 \quad &\text{for all } k \in \{1, \cdots, N-1\}. \end{aligned} \tag{4.4}$$

Given v_k and v_{k-1} in $Q \subset V$, *i.e.*, $g\left(v_k\right) = 0$ and $g\left(v_{k-1}\right) = 0$, we need to solve the following equations

$$\begin{aligned} D_2\mathbb{L}\left(v_{k+1}, v_k\right) + D_1\mathbb{L}\left(v_k, v_{k-1}\right) + \lambda_k^T Dg\left(v_k\right) = 0 \\ g\left(v_{k+1}\right) = 0 \end{aligned} \tag{4.5}$$

for v_{k+1} and λ_k.

In terms of the original, unconstrained Lagrangian, Equation (4.5) reads as follows:

$$\begin{gathered} \frac{1}{h}\left[\frac{\partial L}{\partial \dot{v}}\left(\frac{v_k + v_{k-1}}{2}, \frac{v_k - v_{k-1}}{h}\right) - \frac{\partial L}{\partial \dot{v}}\left(\frac{v_{k+1} + v_k}{2}, \frac{v_{k+1} - v_k}{h}\right)\right] + \\ \frac{1}{2}\left[\frac{\partial L}{\partial v}\left(\frac{v_k + v_{k-1}}{2}, \frac{v_k - v_{k-1}}{h}\right) + \frac{\partial L}{\partial v}\left(\frac{v_{k+1} + v_k}{2}, \frac{v_{k+1} - v_k}{h}\right)\right] + D^T g\left(v_k\right)\lambda_k = 0 \\ g\left(v_{k+1}\right) = 0. \end{gathered} \tag{4.6}$$

For example, if the continuous Lagrangian system is of the form

$$\begin{aligned} L(q, \dot{q}) &= \frac{1}{2}\dot{q}^T M \dot{q} - V(q) \\ g(q) &= 0, \end{aligned} \tag{4.7}$$

where M is a constant mass matrix, and V is the potential energy, then the DEL equations are

$$\begin{gathered} M\left(\frac{v_{k+1} - 2v_k + v_{k-1}}{h^2}\right) + \frac{1}{2}\left(\frac{\partial V}{\partial q}\left(\frac{v_{k+1} + v_k}{2}\right) + \frac{\partial V}{\partial q}\left(\frac{v_k + v_{k-1}}{2}\right)\right) - D^T g\left(v_k\right)\lambda_k = 0 \\ g\left(v_{k+1}\right) = 0. \end{gathered} \tag{4.8}$$

4.2 Generalized Coordinate Formulation

For the generalized coordinate formulation, we form the discrete Lagrangian and the action sum restricted to $Q \subset V$, and then perform the extremization directly on Q by using a coordinate chart. The *constrained, discrete Lagrangian* is given by

$$\mathbb{L}^c : Q \times Q \to \mathbb{R}, \tag{4.9}$$

where $\mathbb{L}^c = \mathbb{L}|_{Q\times Q}$. Given a local coordinate chart, $\psi : U \subset \mathbb{R}^m \to Q \subset V$, where U is an open set in $\mathbb{R}^m$, the *constrained, discrete Lagrangian* is

$$\begin{aligned}\mathbb{L}^c(q_{k+1}, q_k) &= \mathbb{L}(\psi(q_{k+1}), \psi(q_k)) \\ &= L\left(\frac{\psi(q_{k+1}) + \psi(q_k)}{2}, \frac{\psi(q_{k+1}) - \psi(q_k)}{h}\right).\end{aligned}$$

The *constrained action sum* is

$$\mathbb{S}^c = \sum_{k=0}^{N-1} \mathbb{L}^c(q_{k+1}, q_k). \tag{4.10}$$

Extremizing $\mathbb{S}^c : Q^{N+1} \to \mathbb{R}$ gives the discrete Euler-Lagrange (DEL) equations in terms of generalized coordinates,

$$D_2\mathbb{L}^c(q_{k+1}, q_k) + D_1\mathbb{L}^c(q_k, q_{k-1}) = 0. \tag{4.11}$$

In terms of the original, unconstrained Lagrangian, Equation (4.11) equals

$$D^T\psi(q_k)\left\{\frac{1}{h}\left[\frac{\partial L}{\partial \dot{v}}(a_k, d_k) - \frac{\partial L}{\partial \dot{v}}(a_{k+1}, d_{k+1})\right] + \frac{1}{2}\left[\frac{\partial L}{\partial v}(a_k, d_k) + \frac{\partial L}{\partial v}(a_{k+1}, d_{k+1})\right]\right\} = 0, \tag{4.12}$$

where

$$a_k = \frac{\psi(q_k) + \psi(q_{k-1})}{2} \qquad \text{and} \qquad d_k = \frac{\psi(q_k) - \psi(q_{k-1})}{h}. \tag{4.13}$$

We solve Equations (4.12) for q_{k+1} given q_k and q_{k-1} to advance the flow one time step.

4.3 Equivalence of the Formulations

This section proves the equivalence between the constrained and generalized coordinate formulations.

Theorem 4.3.1 *Let g be the constraint function and ψ be the coordinate chart defined above. Let q_k and q_{k-1} be the two initial points in the coordinate chart and let $v_k = \psi(q_k)$ and $v_{k-1} = \psi(q_{k-1})$. Let $Dg(v_k)$ and $D\psi(q_k)$ be full rank. Then the generalized formulation, Equation (4.12), has a solution for q_{k+1} if and only if the constrained formulation, Equation (4.6), has a solution for v_{k+1} and λ_k. Furthermore, $v_{k+1} = \psi(q_{k+1})$.*

Proof ($\Leftarrow$) We assume that we have a solution for v_{k+1} for the constrained formulation. Let $q_{k+1} = \psi^{-1}(v_{k+1})$ and we will show that q_{k+1} solves Equation (4.12). Multiply the top equation in Equation (4.6) on the left by $D^T\psi(q_{k+1})$. Also, substitute $v_k = \psi(q_k)$ and $v_{k-1} = \psi(q_{k-1})$ into Equation (4.6). Notice that $g(\psi(q_k)) = 0$ which implies that $Dg(\psi(q_k))D\psi(q_k) = 0$ and $D^T\psi(q_k)D^Tg(\psi(q_k)) = 0$. Using the substitutions and the fact that $D^T\psi(q_k)D^Tg(\psi(q_k)) = 0$ proves that q_{k+1} is a solution for Equation (4.12).

($\Rightarrow$) To complete the proof, we assume that q_{k+1} is a solution for Equation (4.12) and show that there exists a Lagrange multiplier, λ_k, so that $v_{k+1} = \psi(q_{k+1})$ is a solution for Equation (4.6). Substitute the expressions for v_{k+1}, v_k, and v_{k-1} into Equation (4.6). The lower equation in Equation (4.6) is solved automatically since $v_{k+1} \in Q$. Note that $T_{v_k}V = \mathcal{R}(D\psi(q_k)) \oplus \mathcal{N}(D^T\psi(q_k))$ and that $\mathcal{R}(D^Tg(v_k)) \subset \mathcal{N}(D^T\psi(q_k))$. Since $D^Tg(v_k)$ is full rank and $\dim(\mathcal{R}(D^Tg(v_k))) = \dim(\mathcal{N}(D^T\psi(q_k)))$, $\mathcal{R}(D^Tg(v_k))$ equals $\mathcal{N}(D^T\psi(q_k))$. We then split the left-hand side in Equation (4.6) into a component in $\mathcal{R}(D\psi(q_k))$ and an orthogonal component in $\mathcal{N}(D^T\psi(q_k))$. The component in $\mathcal{R}(D\psi(q_k))$ is zero by Equation (4.12) and the fact that $\mathcal{R}(D^Tg(v_k)) = \mathcal{N}(D^T\psi(q_k))$. We can then find a Lagrange multiplier, λ_k, to make the component in $\mathcal{N}(D^T\psi(q_k))$ equal to zero since $\mathcal{R}(D^Tg(v_k)) = \mathcal{N}(D^T\psi(q_k))$. Therefore, there exists a λ_k so that $v_{k+1} = \psi(q_{k+1})$ solves Equation (4.6). □

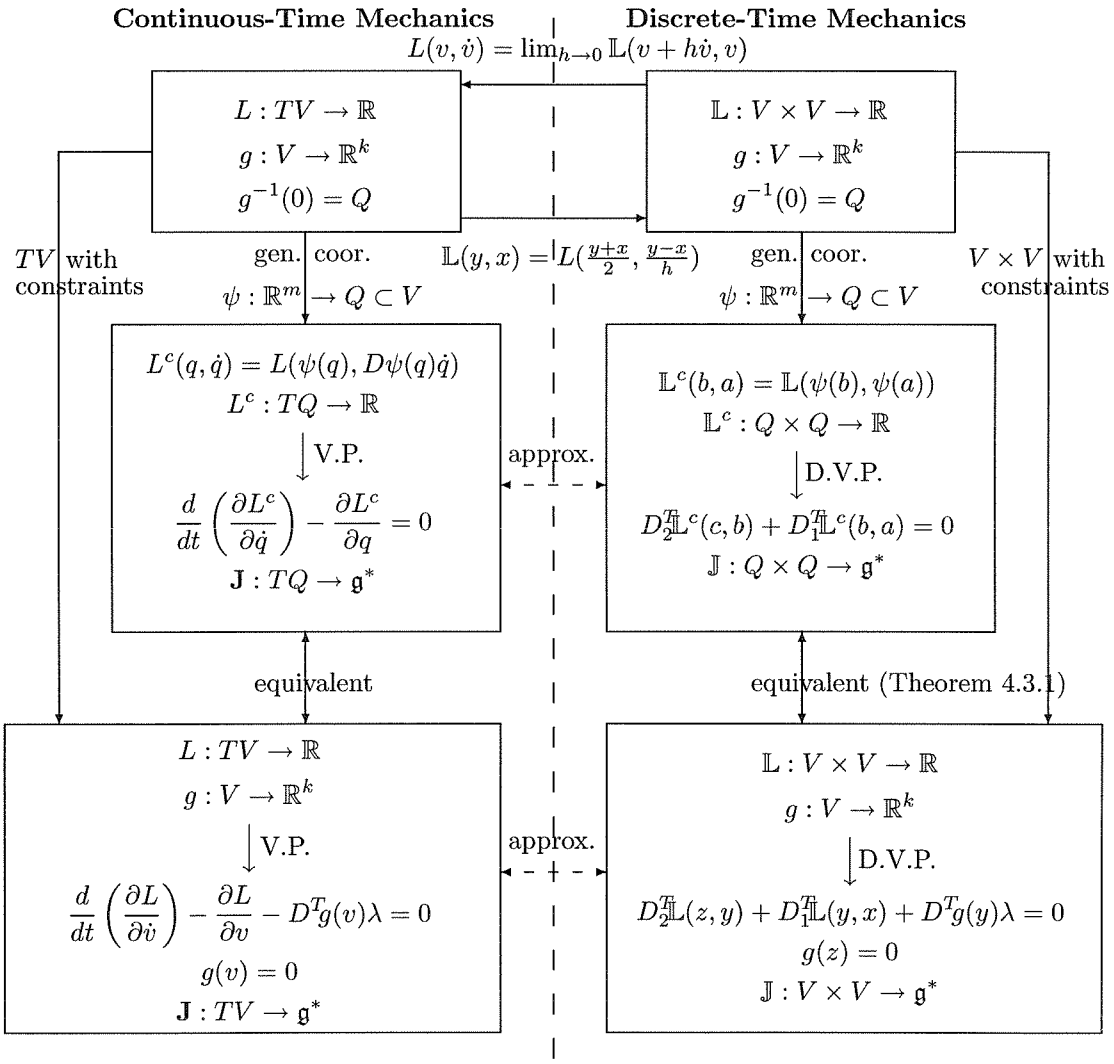

Figure 1: Comparison of Continuous and Discrete Formulations of Mechanics

In Figure 1, we illustrate the relationships between constrained and generalized coordinate formulations for discrete-time mechanics as well as continuous-time mechanics. The figure also points out where the discrete-time equations approximate the flow of the continuous-time equations. The results for continuous-time mechanics are summarized on the left side of the figure. We assume we are given an unconstrained Lagrangian with constraint functions as shown in the upper left corner. One can use generalized coordinates and apply Hamilton's principle to produce the Euler-Lagrange equations or one can use constrained coordinates and enforce the constraints through Lagrange multipliers. The right side of the figure summarizes the results for discrete-time mechanics. Given the continuous, unconstrained Lagrangian, one can form the discrete, unconstrained Lagrangian. One can proceed analogously to continuous-time mechanics by using generalized or constrained coordinates. We discuss in Section 4.5 how the discrete equations approximate the continuous-time equations.

4.4 Jacobian Structure

For the numerical examples presented later in this paper, we solve the DEL equations, Equation (4.5), using Newton-Raphson equation solvers. These solvers require the construction of a Jacobian formed by differentiating Equation (4.5) with respect to v_{k+1} and λ_k to get

$$J(v_{k+1}, v_k, h) = \begin{bmatrix} D_{12}\mathbb{L}(v_{k+1}, v_k) & D^T g(v_k) \\ Dg(v_{k+1}) & 0 \end{bmatrix}, \tag{4.14}$$

where

$$\left[D_{12}\mathbb{L}\left(v_{k+1}, v_k\right)\right]_{ij} = \frac{\partial^2 \mathbb{L}}{\partial v_k^i \partial v_{k+1}^j}\left(v_{k+1}, v_k\right).$$

For many applications, the nearly symmetric Jacobian, Equation (4.14), is a sparse matrix and sparse matrix techniques can be used in the Newton-Raphson steps to increase the simulation efficiency. For tree structured multibody systems, one can show that the linear equations involving the Jacobian can be solved in linear time. Sparse matrix techniques and symplectic integration are also used for multibody systems in (Barth and Leimkuhler, 1996b).

To improve the scaling of the entries in the Jacobian, one can multiply the DEL equations by powers of h. For the rigid body example in Section 5.1, we solve the following equations for v_{k+1} and $\mu_k = h\lambda_k$:

$$\begin{aligned} h^2\left[D_2\mathbb{L}\left(v_{k+1}, v_k\right) + D_1\mathbb{L}\left(v_k, v_{k-1}\right)\right] + \mu_k^T h Dg\left(v_k\right) = 0 \\ hg\left(v_{k+1}\right) = 0 \end{aligned} \tag{4.15}$$

to produce a Jacobian of the form

$$J(v_{k+1}, v_k, h) = \begin{bmatrix} h^2 D_{12}\mathbb{L}(v_{k+1}, v_k) & hD^T g(v_k) \\ hDg(v_{k+1}) & 0 \end{bmatrix}. \tag{4.16}$$

For the double spherical pendulum example, we solve

$$\begin{aligned} h\left[D_2\mathbb{L}\left(v_{k+1}, v_k\right) + D_1\mathbb{L}\left(v_k, v_{k-1}\right)\right] + \mu_k^T Dg\left(v_k\right) = 0 \\ g\left(v_{k+1}\right) = 0 \end{aligned} \tag{4.17}$$

to produce a Jacobian of the form

$$J(v_{k+1}, v_k, h) = \begin{bmatrix} hD_{12}\mathbb{L}(v_{k+1}, v_k) & D^T g(v_k) \\ Dg(v_{k+1}) & 0 \end{bmatrix}. \tag{4.18}$$

4.5 Local Truncation Error and Solvability

Results on truncation error and solvability are presented in this section. To calculate the truncation error, we first insert an exact solution of the differential equations into the algorithm equations in Equation (4.12), and then expand the resulting equation in terms of the step size h. To calculate the expansion, it is easier to first expand Equation (4.12) about

$$v_k^i = \psi^i(q_k) \qquad \text{and} \qquad \dot{v}_k^i = \frac{\partial \psi^i}{\partial q_k^j}\dot{q}_k^j, \tag{4.19}$$

and then expand the result into powers of h. This lengthy calculation which we do not reproduce here reveals that the local truncation error of the method is second order. The first term, h^0, is zero since $q, \dot{q}$ satisfy the continuous Euler-Lagrange equations. The second term, h^1, is zero through a cancellation of terms. The h^2 term is non-zero, and the coefficient is a lengthy expression involving second, third, and fourth partial derivatives of $L : TV \to \mathbb{R}$.

If one uses the following definition for the discrete Lagrangian:

$$\mathbb{L}(y, x) = L(y, \frac{y - x}{h}), \tag{4.20}$$

then the resulting DEL equations will only be first order accurate for a general Lagrangian. There is no cancellation of terms in the h^1 term as there is with the definition in Equation (4.1). However, in some cases, the resulting DEL equations may be explicit while the DEL equations from the definition in Equation (4.1) are implicit. An example of this occurring is if the continuous Lagrangian is in the form in Equation (4.7), and there are no constraints.

The existence of a solution for the continuous-time equations is related to the solvability of the generalized coordinate discrete equations. One can show that if $D_{22}L$ is non-singular and if the Jacobian of the constraints is full rank, then for a sufficiently small time step, the generalized coordinate DEL equations are solvable for q_{k+1}. This is proved by showing that the DEL equations have a solution for $h = 0$ by taking the limit and then by using the implicit function theorem to conclude that there is a solution in a neighborhood of $h = 0$. Theorem 4.3.1 then implies that there is also a solution for the DEL equations with Lagrange multipliers.

4.6 Symplectic Form and Discrete Momentum Map

The integrators created through the construction procedure are symplectic-momentum integrators, however, this statement requires clarification which we present in this section. The integrators are symplectic in that the map produced on T^*V or T^*Q is a symplectic map. Also, if the Lie group acts linearly on V, then the continuous flow of the Euler-Lagrange equations and the discrete map produced from the DEL equations preserve the same momentum map on T^*Q.

However, if one integrates the continuous equations exactly or accurately and uses the result to initialize the discrete equations, one will notice that the *value* of the momentum map will differ from the value of the momentum map for the continuous system. The difference arises from the difference in the assignment of the momentum coordinate in T^*V through the fiber derivative. In the continuous case, the momentum is D_2L while in the discrete case, we choose to use $-hD_2\mathbb{L}$. We multiply by a $-h$ from the definitions given in Equation (3.1) because $-hD_2\mathbb{L}$ converges to D_2L as $h \to 0$.

If the Lagrangian of a continuous system is invariant to the action of a group, and if the constraints are also invariant under the group action, *i.e.*

$$\begin{gathered} L : TV \to \mathbb{R} \\ L\left(G \cdot v, G \cdot \dot{v}\right) = L\left(v, \dot{v}\right) \\ g\left(G \cdot v\right) = g\left(v\right), \end{gathered}$$

where the action of G on $v \in V$ is represented as $G \cdot v$, then the flow of the Euler-Lagrange equations preserve the momentum map,

$$\mathbf{J} : TV \to \mathfrak{g}^*,$$

where

$$\langle \mathbf{J}(v,\dot{v}),\xi\rangle \triangleq \left\langle \frac{\partial L}{\partial \dot{v}}(v,\dot{v}),\xi_V(v)\right\rangle.$$

If the group G also acts linearly on V, then the discrete Lagrangian is also invariant to the group action through the following calculation:

$$\begin{aligned}\mathbb{L}(G\cdot v_{k+1},G\cdot v_k) &= L\left(\frac{G\cdot v_{k+1}+G\cdot v_k}{2},\frac{G\cdot v_{k+1}-G\cdot v_k}{h}\right)\\ &= L\left(G\cdot\left(\frac{v_{k+1}+v_k}{2}\right),G\cdot\left(\frac{v_{k+1}-v_k}{h}\right)\right)\\ &= L\left(\frac{v_{k+1}+v_k}{2},\frac{v_{k+1}-v_k}{h}\right)\\ &= \mathbb{L}(v_{k+1},v_k).\end{aligned}$$

From a similar derivation to the derivation in Section (3.3), one can show that the following momentum map

$$\mathbb{J}: V\times V\to \mathfrak{g}^*$$

defined by the relation

$$\langle \mathbb{J}(v_{k+1},v_k),\xi\rangle \triangleq \langle D_2\mathbb{L}(v_{k+1},v_k),\xi_V(v_k)\rangle$$

is conserved by the flow of the DEL equations.

We now calculate $-hD_2\mathbb{L}$ and notice

$$\begin{aligned}-hD_2\mathbb{L}(v_{k+1},v_k) &= -h\frac{\partial}{\partial v_k}\left(L\left(\frac{v_{k+1}+v_k}{2},\frac{v_{k+1}-v_k}{h}\right)\right)\\ &= \frac{\partial L}{\partial \dot{v}}\left(\frac{v_{k+1}+v_k}{2},\frac{v_{k+1}-v_k}{h}\right)-\frac{h}{2}\frac{\partial L}{\partial v}\left(\frac{v_{k+1}+v_k}{2},\frac{v_{k+1}-v_k}{h}\right).\end{aligned}$$

As $h\to 0$, the discrete momentum value, $-hD_2\mathbb{L}$, converges to the continuous momentum value, D_2L. Therefore, the quantities that depend on the discrete momentum value, such as the *discrete momentum map* defined to be $-h\mathbb{J}$, converge to their continuous counterparts as $h\to 0$.

5 Numerical Examples

We apply the construction procedure to produce mechanical integrators for the rigid body (RB) and the double spherical pendulum (DSP). We choose to use constrained coordinates instead of generalized coordinates to avoid coordinate singularities and coordinate patching. We use unit quaternions to create the rigid body algorithm, and use the position of the two masses for the double spherical pendulum. We compare the double spherical pendulum algorithm to an energy-momentum algorithm presented in (Wendlandt, 1995) based on the work in (Gonzalez, 1996a).

5.1 Rigid Body

The algorithm presented here updates quaternion variables based on the previous two quaternion variables. The configuration manifold is taken to be $Q=S^3\subset V$ where $V=\mathbb{R}^4$. Quaternions were used instead of using $V=\mathbb{R}^9$ with the six orthogonal constraints of $SO(3)$ primarily to avoid a large number of Lagrange multipliers. The constraint function is $g(v)=v\cdot v-1$ and is enforced with Lagrange multipliers.

Rigid body integrators that preserve certain mechanical properties have been created by several researchers. A symplectic integrator which preserves the momentum and energy is presented in (Lewis and

Simo, 1995). An energy-momentum integrator is presented in (Simo and Wong, 1991). A symplectic-momentum integrator is presented in (McLachlan and Scovel, 1995). A rigid body integrator based on a discrete variational principle and in terms of 3×3 matrices with constraints is presented in (Moser and Veselov, 1991). It would be interesting to compare in more detail the integrator in (Moser and Veselov, 1991) to the quaternion-based integrator in this section.

We first attach a body frame to the rigid body and represent the frame as a matrix, $R \in SO(3)$, which maps vectors in the body frame, $\mathcal{B}$, to vectors in the spatial (inertial) frame, $\mathcal{S}$. The rotation matrix is then thought of as a mapping, $R : \mathcal{B} \to \mathcal{S}$.

We now present a background in quaternions. Consult (Murray et al., 1994) for more information on quaternions. A unit quaternion is a four parameter representation of $SO(3)$. The quaternion consists of a scalar value, q_s, and a vector with three components which we denote $q_v = (q_x, q_y, q_z)$. The following formula constructs a $SO(3)$ matrix, A, from its unit quaternion representation, a:

$$A = (2a_s^2 - 1)I + 2a_s\hat{a}_v + 2a_v a_v^T, \tag{5.1}$$

where

$$\hat{a}_v = \begin{bmatrix} 0 & -a_z & a_y \\ a_z & 0 & -a_x \\ -a_y & a_x & 0 \end{bmatrix}. \tag{5.2}$$

A useful property of the unit quaternion representation is that if A, B, and $C \in SO(3)$ are represented by unit quaternions, a, b, and c, respectively, then $C = AB$ if and only if $c = \pm a \star b$ where $\star$ represents quaternion multiplication. If $c = a \star b$, then $c_s = a_s \star b_s - a_v \cdot b_v$ and $c_v = a_s b_v + b_s a_v + a_v \times b_v$. Also, the conjugate of a denoted $\bar{a}$ is given by $\bar{a} = (a_s, -a_v)$. For unit quaternions, $\bar{a}$ is the inverse of a, in that $a \star \bar{a} = (1, 0, 0, 0)$. An additional fact about quaternions is that if $w = Av$ and a is a unit quaternion that represents A, then $(0, w) = a \star (0, v) \star \bar{a}$ where $(0, w)$ is a quaternion formed from the vector w.

If $R : \mathcal{B} \to \mathcal{S}$ is the rotation matrix representing the orientation of the rigid body, then the body angular velocity vector, ω_b, is given by $\hat{\omega}_b = R^T\dot{R}$. Another fact about quaternions is that if r is the unit quaternion representing R, then $\bar{r} \star \dot{r} = (0, \omega_b/2)$.

Using the above relationship for the body angular velocity, we construct the continuous Lagrangian, $L : TV \to \mathbb{R}$, to be

$$L(q, \dot{q}) = \frac{1}{2}(2\overline{q} \star \dot{q})^T \begin{bmatrix} 0 & 0 \\ 0 & \mathbb{I} \end{bmatrix} (2\overline{q} \star \dot{q}), \tag{5.3}$$

where $\mathbb{I}$ is the inertia matrix. The constraint is the unit norm constraint for quaternions, $q_s^2 + q_v \cdot q_v = 1$.

The Lagrangian in Equation (5.3) is invariant under left quaternionic multiplication, *i.e.*

$$L(r \star q, r \star \dot{q}) = L(q, \dot{q}),$$

where r is a unit quaternion. The invariance leads to conservation of angular momentum.

The discrete Lagrangian, $\mathbb{L} : TV \to \mathbb{R}$, is chosen to be

$$\mathbb{L}(y, x) = L\left(\frac{y+x}{2}, \frac{y-x}{h}\right). \tag{5.4}$$

We first simplify the body angular velocity term to get

$$2\overline{q} \star \dot{q} \mapsto \left(\overline{\frac{y+x}{2}}\right) \star \left(\frac{y-x}{h}\right) \tag{5.5}$$

$$= \frac{1}{h}(\overline{y} \star y - \overline{y} \star x + \overline{x} \star y - \overline{x} \star x). \tag{5.6}$$

Restricted to Q, $\overline{y} \star y = \overline{x} \star x = (1,0,0,0)$. Simplifying restricted to Q gives

$$2\overline{q} \star \dot{q} \mapsto \frac{1}{h}(\overline{x} \star y - \overline{y} \star x). \tag{5.7}$$

Equation (5.7) is an approximation to the body angular velocity, $(0, \omega_b)$. The simplified discrete Lagrangian restricted to Q is then

$$\mathbb{L}(y,x) = \frac{1}{2h^2}(\overline{x} \star y - \overline{y} \star x)^T \begin{bmatrix} 0 & 0 \\ 0 & \mathbb{I} \end{bmatrix} (\overline{x} \star y - \overline{y} \star x), \tag{5.8}$$

and the discrete Lagrangian on all of $V \times V$ is then taken to be equal to Equation (5.8). Since we are extremizing $\mathbb{S}$ restricted to Q, the extension of $\mathbb{L}$ to $V \setminus Q$ is arbitrary.

The discrete Lagrangian in Equation (5.8) is also invariant under left quaternionic multiplication, *i.e.*

$$\mathbb{L}(r \star y, r \star x) = \mathbb{L}(y,x),$$

where r is a unit quaternion, and the invariance leads to conservation of discrete momentum which converges to the continuous momentum as the step size decreases, as we have seen.

The DEL equations for the RB and relevant Jacobian are created in Mathematica (Wolfram, 1991) and exported to C-code for simulation. The initial conditions and RB parameters are

$$q_0 = \begin{bmatrix} 1 \\ 0 \\ 0 \\ 0 \end{bmatrix} \qquad \omega_b = \begin{bmatrix} 0 \\ 3 \\ 4 \end{bmatrix} \qquad \mathbb{I} = \begin{bmatrix} 1 & 0 & 0 \\ 0 & 2 & 0 \\ 0 & 0 & 3 \end{bmatrix}. \tag{5.9}$$

We must first initialize the rigid body integrator by choosing two initial quaternion values. We do this by using an Euler step with $\dot{q} = q \star (0, \omega_b/2)$ with $h = 10^{-5}$s. We then use the DVP integrator with $h = 10^{-5}$s to set the second initial point for $h = 10^{-4}$s, 10^{-3}s, 10^{-2}s, and 10^{-1}s. The system is simulated for 30 seconds. To calculate errors in energy, momentum, and position, we first choose a standard value. We use the energy and momentum given initially after the first Euler step at $h = 10^{-5}$s as the standard energy and momentum values. We use the results of the 30s simulation with $h = 10^{-4}$s as the standard position variables. We use the following formula to calculate errors for each simulation:

$$\text{error} = \frac{1}{Nm} \sum_{i=1}^{N} \parallel v_i - v_i^s \parallel_2, \tag{5.10}$$

where m is the length of the vector v_i, v_i^s is the standard value at the ith sample, and N is the number of samples. The results of the simulations are tabulated in Table 1. The table lists CPU time on a SGI Indy

h (s)	CPU time (s)	Quaternion Error	Energy Error	Momentum Error
0.0001	97.620	0.0	0.00000062559469	0.00000016714624
0.001	9.905	0.00000395996880	0.00006274300332	0.00001686683194
0.01	1.397	0.00039966872027	0.00627440600000	0.00168665680795
0.1	0.301	0.03647626533327	0.62167959600000	0.16652140510229

Table 1: Simulation Results for the Rigid Body Simulation

(1 100 MHZ IP22 Processor, FPU: MIPS R4610 Floating Point, CPU:MIPS R4600 Processor), quaternion error, energy error, and momentum error.

Figure 2 is a log-log plot of CPU time in seconds versus time step in seconds. The CPU time drops off nearly linearly as the time step increases. The CPU time is corrected for the time it takes to initialize each simulation with the $h = 10^{-5}$s simulation.

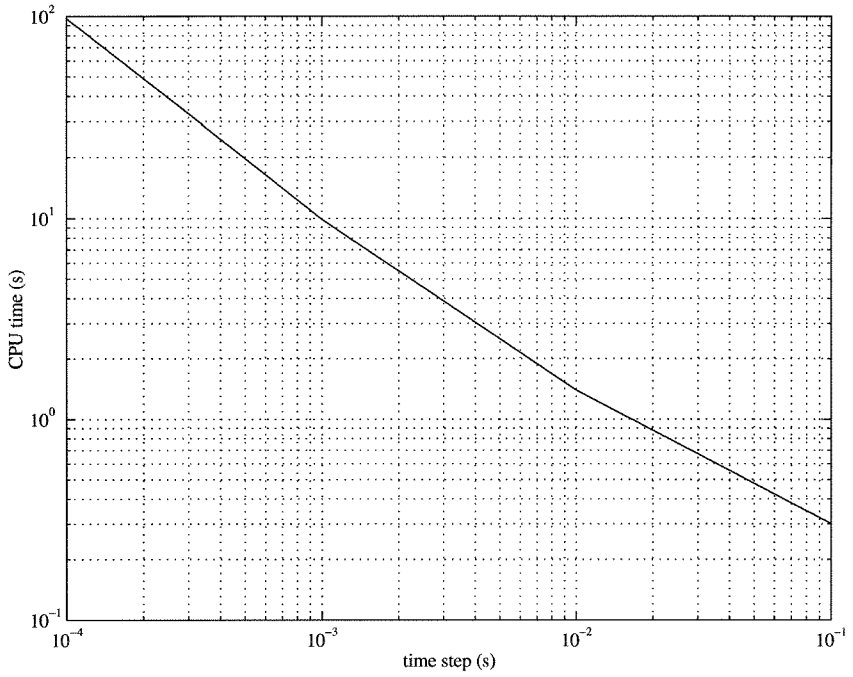

Figure 2: CPU Time Versus Time Step for the Rigid Body Simulation

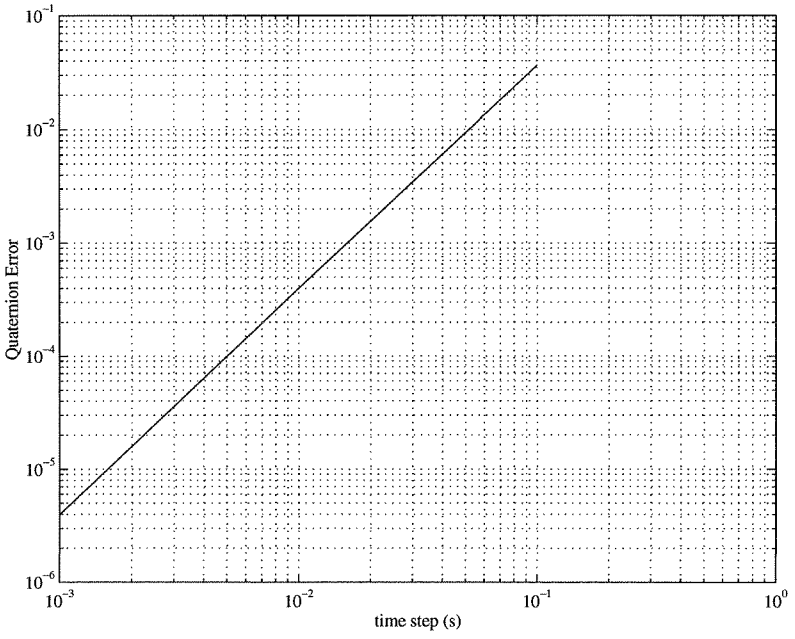

Figure 3: Quaternion Error Versus Time Step

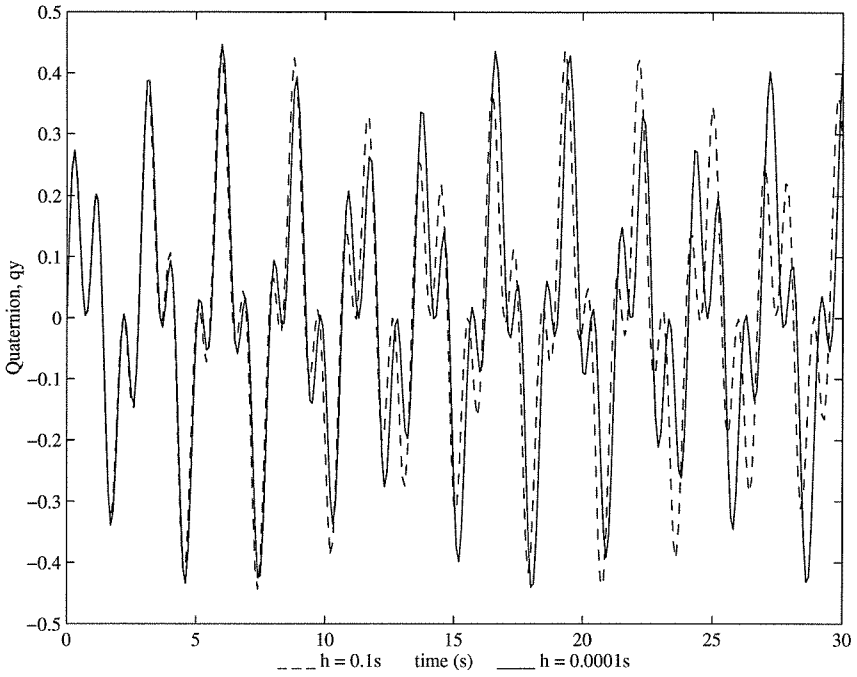

Figure 4: Quaternion Coordinate Versus Time

The quaternion error versus time step is shown in Figure 3. The plot shows a second order relationship between error and time step.

Figure 4 compares the plot of the quaternion, q_y, versus time for the simulations at $h = 10^{-4}$s and $h = 10^{-1}$s. The trajectory for the large time step exhibits the same qualitative behavior as the small time step, but the deviations increase for longer simulation times.

The energy error versus time step is shown in Figure 5. The figure reveals a second order relationship between energy error and time step. The energy for the $h = 10^{-4}$s simulation deviates between 32.999999359J and 32.999999349J. The energy for the simulation at $h = 10^{-3}$s deviates between 32.999937236J and 32.999937235J. There is no deviation in energy for the $h = 10^{-2}$s and $h = 10^{-1}$s simulations.

For each time step, the constant value of the discrete momentum map is conserved, however, as explained in Section 4.6, the value converges to the continuous momentum value as the step size decreases. The convergence of the discrete momentum is shown in Figure 6. The figure reveals a second order relationship between momentum error and time step. The angular momentum for each simulation should remain constant, but there are small deviations ($\pm 10^{-9}$) in the data for the $h = 10^{-4}$s simulation. There are no deviations in the momentum value for the other simulations.

5.2 Double Spherical Pendulum

The double spherical pendulum consists of two constrained point masses. The configuration space is $Q = S^2 \times S^2$ and the linear space is $V = \mathbb{R}^3 \times \mathbb{R}^3$. The position of the first mass is $q_1 = (x_1, y_1, z_1)$, and the position of the second mass is $q_2 = (x_2, y_2, z_2)$. The constraint equation, given by the pendulum length constraints, is

$$g(v) = \begin{bmatrix} q_1 \cdot q_1 - l_1^2 \\ (q_2 - q_1) \cdot (q_2 - q_1) - l_1^2 \end{bmatrix}. \tag{5.11}$$

The DSP Lagrangian system is of the form in Equation (4.7), and the DEL equations for this system are

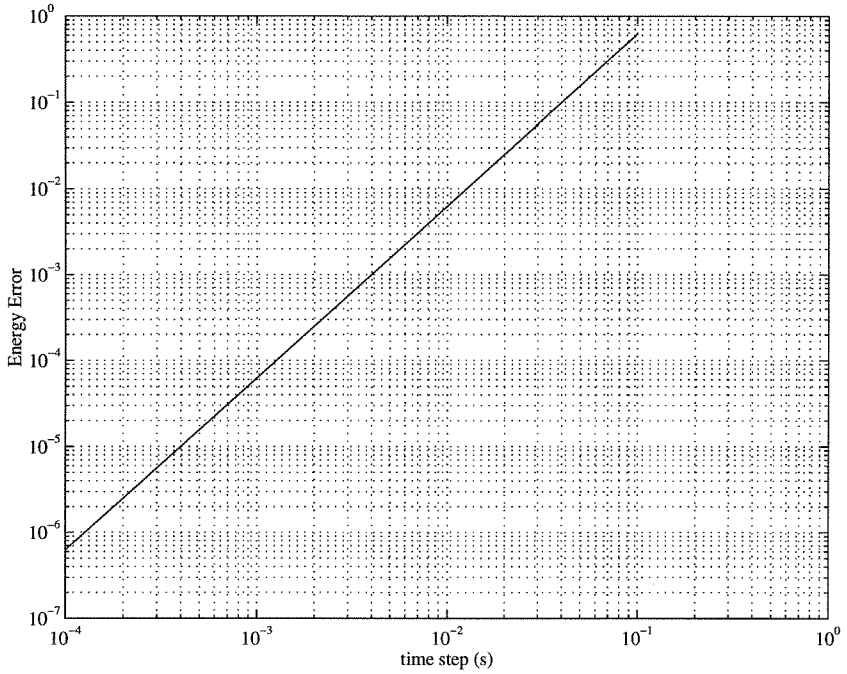

Figure 5: Energy Error Versus Time Step for the Rigid Body Simulation

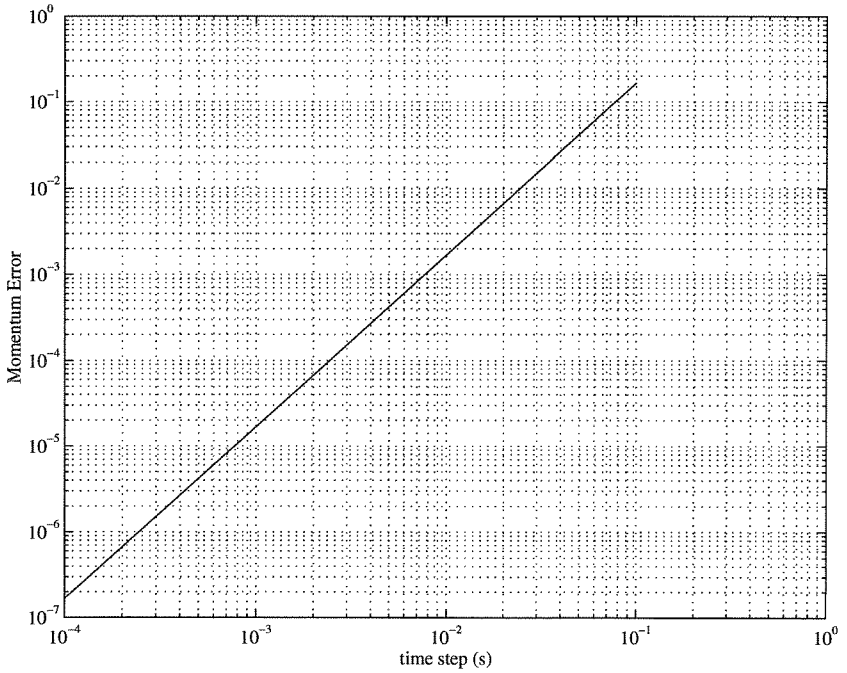

Figure 6: Momentum Error Versus Time Step for the Rigid Body Simulation

of the form in Equation (4.8). The DVP algorithm for the DSP is the SHAKE algorithm:

$$\frac{1}{h}M\left[q^{n+1}-2q^n+q^{n-1}\right]+h\begin{bmatrix}0\\0\\m_1g\\0\\0\\m_2g\end{bmatrix}+hD^Tg\left(q^n\right)\lambda=0$$
$$g\left(q^{n+1}\right)=0,$$

where

$$M=\begin{bmatrix}m_1I & 0\\ 0 & m_2I\end{bmatrix},\qquad q=\begin{bmatrix}q_1\\q_2\end{bmatrix}, \tag{5.12}$$

and m_1 and m_2 are the masses.

We compare the simulation from the discrete variational principle (DVP) construction to an energy-momentum (EM) formulation based on the construction procedure in (Gonzalez, 1996a), and applied to the DSP in (Wendlandt, 1995). The EM algorithm for the DSP is

$$q_1^{n+1}-q_1^n-h\frac{1}{m_1}p_1^{n+\frac{1}{2}}=0$$
$$q_2^{n+1}-q_2^n-h\frac{1}{m_2}p_2^{n+\frac{1}{2}}=0$$
$$p^{n+1}-p^n+h\left[\begin{bmatrix}0\\0\\m_1g\\0\\0\\m_2g\end{bmatrix}+\lambda_1\begin{bmatrix}q_1^{n+1}+q_1^n\\0\end{bmatrix}+\lambda_2\begin{bmatrix}q_1^{n+1}+q_1^n-q_2^{n+1}-q_2^n\\q_2^{n+1}+q_2^n-q_1^{n+1}-q_1^n\end{bmatrix}\right]=0$$
$$\left(q_1^{n+1}\right)\cdot\left(q_1^{n+1}\right)-l_1^2=0$$
$$\left(q_2^{n+1}-q_1^{n+1}\right)\cdot\left(q_2^{n+1}-q_1^{n+1}\right)-l_2^2=0,$$

where p_i is the momentum for the ith mass, p is the six vector of momentum formed by stacking p_1 and p_2, and

$$p_i^{n+\frac{1}{2}}=\frac{1}{2}\left(p_i^{n+1}+p_i^n\right).$$

The following parameters are used for the DSP: $m_1=2.0$Kg, $m_2=3.5$Kg, $l_1=4.0$m, $l_2=3.0$m, and $g=9.81\text{m/s}^2$. The initial conditions are $x_1=2.820$m, $y_1=0.025$m, $x_2=5.085$m, $y_2=0.105$m, $\dot{x}_1=3.381$m/s, $\dot{y}_1=2.506$m/s, $\dot{x}_2=2.497$m/s, and $\dot{y}_2=10.495$m/s. The position and velocity of the z-coordinate is determined from the constraints, and the z-coordinate for both masses is taken to be negative. The output of the EM simulation at a time step of 0.0001s is used as the standard and initializes the second step in the DVP simulations. The results of the EM simulations and the DVP simulations are summarized in Table 2. The table contains the CPU time, position error, energy error and momentum error for the EM and the DVP simulations. The energy and momentum error for the EM simulations are zero. Equation (5.10) is used to calculate the errors for the DSP simulations.

Figure 7 is a plot of CPU time versus time step for the EM and DVP simulations. The DVP simulations are slightly faster for each time step and both CPU times drop off nearly linearly with increasing time step.

The position error for the EM and DVP simulations is shown in Figure 8. Both simulations show a second order relationship between position error and time step. The error for the EM simulation is slightly greater than the error for the DVP simulation for $h\geq 10^{-3}$s.

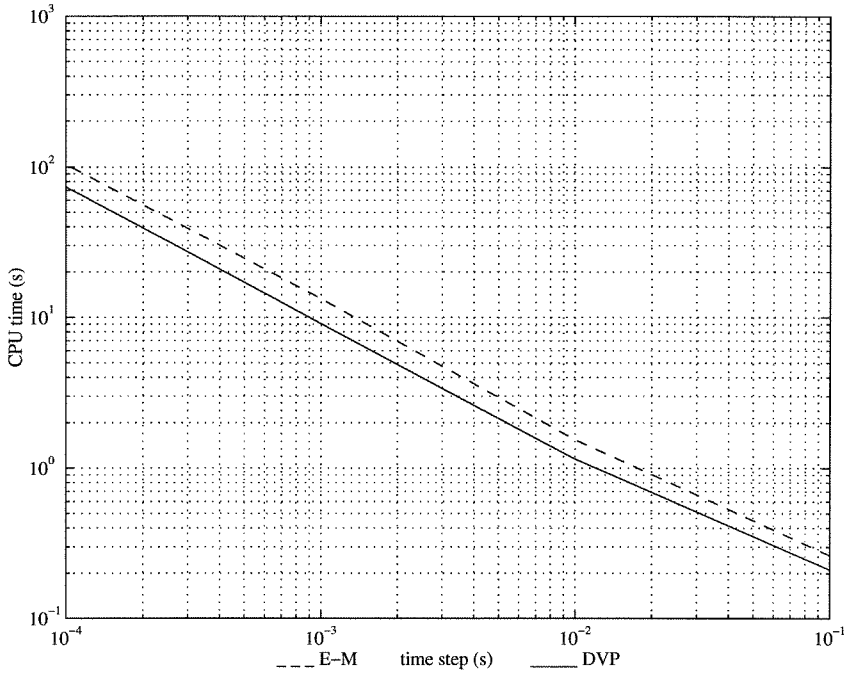

Figure 7: CPU Time Versus Time Step for the DSP Simulation

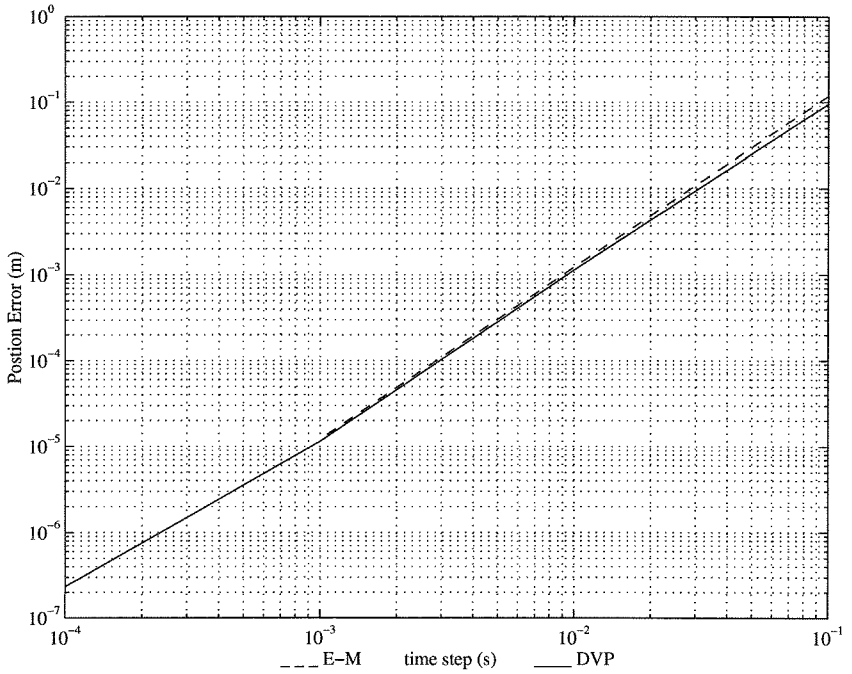

Figure 8: Position Error Versus Time Step for the DSP Simulation

h (s)	Method	CPU time (s)	Position Error	Energy Error	Momentum Error
0.0001	DVP	73.648	0.00000023292428	0.00000647521262	0.00000254701662
	EM	103.871	0.0	0.0	0.0
0.001	DVP	9.065	0.00001146362264	0.00032685721927	0.00017074600001
	EM	13.250	0.00001214070733	0.0	0.0
0.01	DVP	1.152	0.00113498458508	0.03223741607973	0.01696175300000
	EM	1.549	0.00122489163701	0.0	0.0
0.1	DVP	0.211	0.09575837631416	2.66479215701329	1.55996134500002
	EM	0.263	0.11843736345452	0.0	0.0

Table 2: Simulation Results for the DSP Simulation

The y position of the second mass is shown in Figure 9 for the EM and DVP simulations for $h = 0.0001$s and $h = 0.1$s. Both the EM and DVP simulations at $h = 0.0001$s overlap and cannot be distinguished when plotted on the same graph. For both the EM and DVP simulations, reasonably accurate and fast trajectories are produced at large time steps, $h = 0.1$s. Both simulation methods may have uses in interactive simulation applications, such as design and animation, where real-time, reasonably accurate simulations are important.

The error in energy versus time step is shown in Figure 10. The DVP energy error appears to drop off as the square of the time step, at least for the large time steps. The energy error is zero for all time steps for the EM simulation. The energy for the DVP simulation at $h = 0.0001$s deviates between 24.944495109J and 24.944499828J and deviates between 20.910805793J and 25.583335766J for $h = 0.1$s.

The error in the momentum about the z-axis is shown in Figure 11. The momentum error for the EM simulation is zero for all time steps. The DVP algorithm should preserve momentum but for the smallest time step, $h = 0.0001$s, the momentum varies between 199.8254671<u>70</u>m^2/s to 199.8254671<u>84</u>m^2/s. The variation may be due to numerical errors. The momentum is constant for the other time steps. Again, the constant discrete momentum value approaches the value of the continuous momentum as the step size decreases.

Figure 12 shows the energy for the DVP simulations versus time for $h = 0.1$s and 0.01s in the lower graph. The upper graph shows energy versus time for $h = 0.001$s and 0.0001s. The energy oscillates about a constant value, and the constant value approaches the true energy. The amplitude of the oscillations decrease as the step size decreases. The fluctuations in energy appear to be related to the constraint forces. The middle graph is a plot of the multipliers versus time, and the fluctuations in the multipliers is correlated to the fluctuations in energy. This relationship has also been noticed in (Barth and Leimkuhler, 1996a), and they use variable step size to decrease the energy oscillation.

6 Conclusion

This paper presented a procedure to construct mechanical integrators for Lagrangian systems and applied the method to the rigid body and the double spherical pendulum. The discrete Euler-Lagrange (DEL) equations share similarities to the continuous equations of motion and preserve a symplectic form and invariants resulting from group invariance of the Lagrangian.

There are many areas of future work and development. We list a few of these here.

Energy-Momentum Integrators. One may proceed analogously to the derivation in this paper to create energy-momentum integrators possibly based on discretizing the principle of least action.

Nonholonomic Systems. The method presented in this paper treats holonomic constraints and one would like to generalize the method to treat nonholonomic constraints, as in (Bloch et al., 1996). For nonholonomic systems, the standard symplectic form is not preserved, and there are momentum equations and not conservation laws. Also, energy can be conserved in these systems. One has to develop algorithms taking into account these effects.

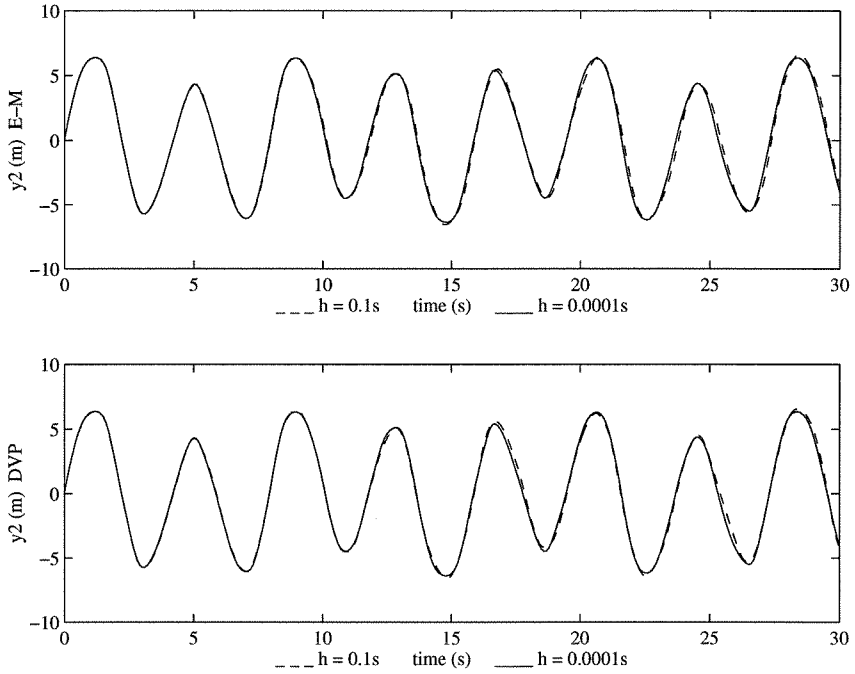

Figure 9: Position Coordinate Versus Time for the DSP Simulation

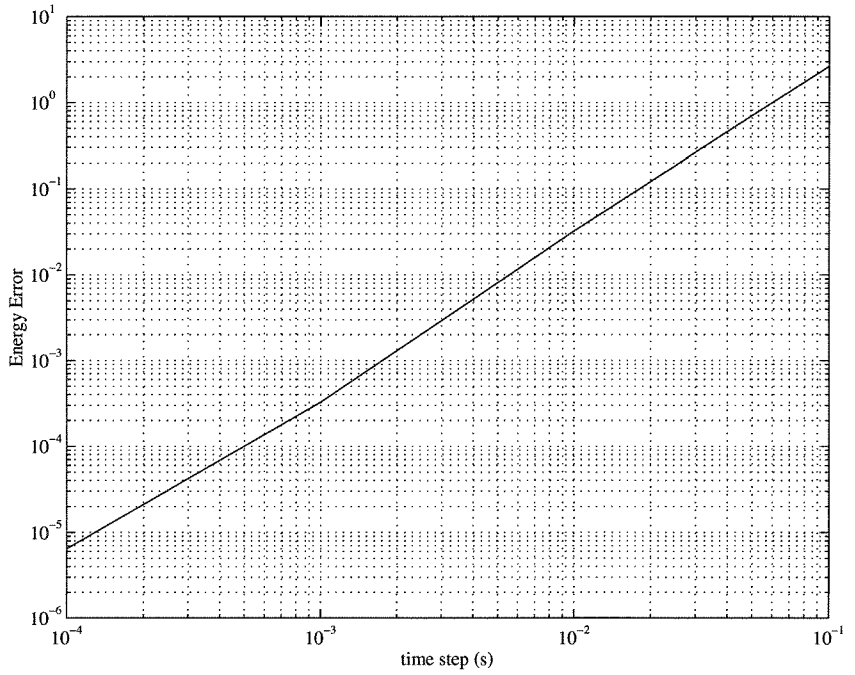

Figure 10: Energy Error Versus Time Step for the DSP Simulation

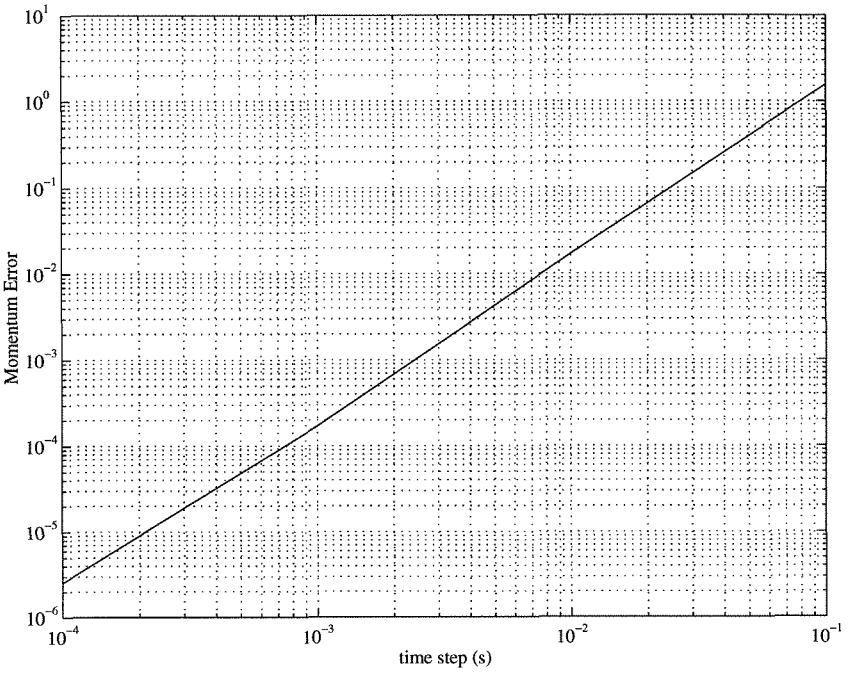

Figure 11: Momentum Error Versus Time Step for the DSP Simulation

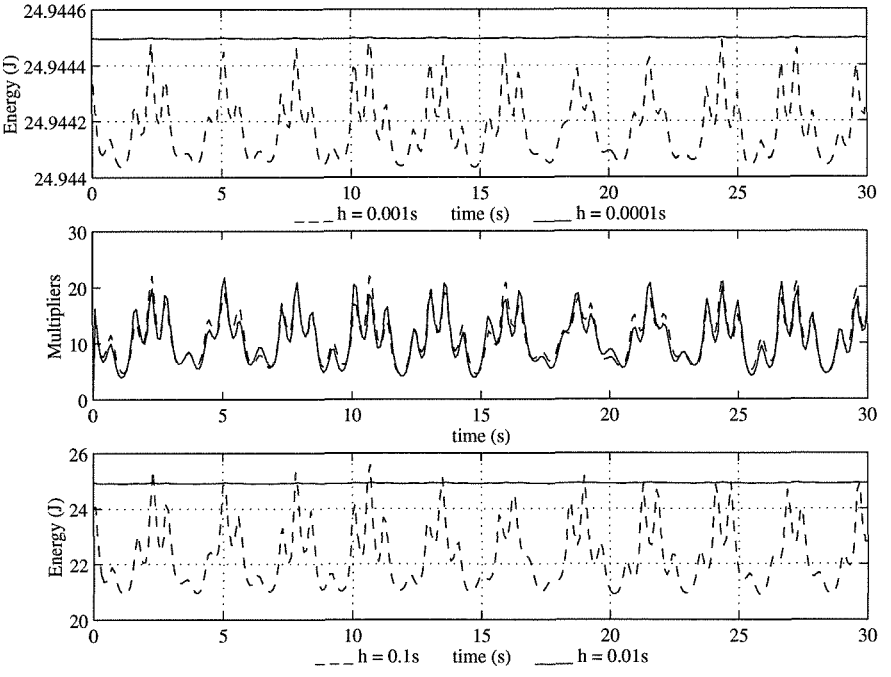

Figure 12: Energy and Multipliers Versus Time for the DSP Simulation

Multistep Methods and Time Step Control. It seems possible to modify the method to construct multistep mechanical integrators to increase the accuracy of the method. One would also like to modify the method to allow variable time steps to improve efficiency.

External Forces. It would also be desirable to generalize the method to include external forces. This should be straightforward since they can be included in Hamilton's principle in standard fashion. One would also like to add control forces and dissipative forces to simulate controlled mechanical systems. The first author is currently using the techniques presented in this paper to develop a multibody simulator to simulate control systems for human models (Wendlandt and Sastry, 1996).

Spacetime Integrators Since the method here is variational by nature and focuses on the temporal behavior, it should be helpful in the development of spacetime integrators by synthesis with existing finite element methods.

Acknowledgements

We first would like to thank Andrew Lewis for pointing out (Baez and Gilliam, 1995). We would also like to thank Richard Murray and Abhi Jain for help with an initial investigation into mechanical integrators. We appreciate the useful comments and discussions provided by Francisco Armero and Oscar Gonzalez. We also thank Robert MacKay and Shmuel Weissman for useful discussions.

References

Anderson, H. (1983). Rattle: A velocity version of the shake algorithm for molecular dynamics calculations. *Journal of Computational Physics*, 52:24–34.

Armero, F. and Simo, J. (1996). Long-term dissipativity of time-stepping algorithms for an abstract evolution equation with applications to the incompressible mhd and navier-stokes equations. *Computer Methods in Applied Mechanics and Engineering*, 131(1-2):41–90.

Baez, J. C. and Gilliam, J. W. (1995). An algebraic approach to discrete mechanics. Preprint, http://math.ucr.edu/home/baez/ca.tex.

Barth, E. and Leimkuhler, B. (1996a). A semi-explicit, variable-stepsize integrator for constrained dynamics. Mathematics department preprint series, University of Kansas.

Barth, E. and Leimkuhler, B. (1996b). Symplectic methods for conservative multibody systems. *Fields Institute Communications*, 10:25–43.

Bloch, A., Krishnaprasad, P., Marsden, J., and Murray, R. (1996). Nonholonomic mechanical systems with symmetry. *Archive for Rational Mechanics and Analysis.* To appear.

Channell, P. and Scovel, C. (1990). Symplectic integration of hamiltonian systems. *Nonlinearity*, 3:231–259.

Chorin, A., Hughes, T., Marsden, J., and McCracken, M. (1978). Product formulas and numerical algorithms. *Comm. Pure Appl. Math.*, 31:205–256.

Ge, Z. and Marsden, J. (1988). Lie-poisson integrators and lie-poisson hamilton-jacobi theory. *Phys. Lett. A*, 133:134–139.

Gillilan, R. and Wilson, K. (1992). Shadowing, rare events, and rubber bands. a variational verlet algorithm for molecular dynamics. *J. Chem. Phys.*, 97(3):1757–1772.

Gonzalez, O. (1996a). *Design and Analysis of Conserving Integrators for Nonlinear Hamiltonian Systems with Symmetry.* Ph.D. thesis, Stanford University. Department of Mechanical Engineering.

Gonzalez, O. (1996b). Time integration and discrete hamiltonian systems. *Journal of Nonlinear Science*. To appear.

Itoh, T. and Abe, K. (1988). Hamiltonian-conserving discrete canonical equations based on variational difference quotients. *Journal of Computational Physics*, 77:85–102.

Jay, L. (1996). Symplectic partitioned runge-kutta methods for constrained hamiltonian systems. *SIAM Journal on Numerical Analysis*, 33(1):368–87.

Labudde, R. A. and Greenspan, D. (1974). Discrete mechanics-a general treatment. *Journal of Computational Physics*, 15:134–167.

Labudde, R. A. and Greenspan, D. (1976a). Energy and momentum conserving methods of arbitrary order for the numerical integration of equations of motion-i. motion of a single particle. *Numer. Math.*, 25:323–346.

Labudde, R. A. and Greenspan, D. (1976b). Energy and momentum conserving methods of arbitrary order for the numerical integration of equations of motion-ii. motion of a system of particles. *Numer. Math.*, 26:1–16.

Leimkuhler, B. and Patrick, G. (1996). Symplectic integration on riemannian manifolds. *Journal of Nonlinear Science*. To appear.

Leimkuhler, B. and Skeel, R. (1994). Symplectic numerical integrators in constrained hamiltonian systems. *Journal of Computational Physics*, 112:117–125.

Lewis, D. and Simo, J. (1995). Conserving algorithms for the dynamics of hamiltonian systems on lie groups. *Journal of Nonlinear Science*, 4:253–299.

Lewis, H. and Kostelec, P. (1996). The use of hamilton's principle to derive time-advance algorithms for ordinary differential equations. *Computer Physics Communications*. To appear.

MacKay, R. (1992). Some aspects of the dynamics of hamiltonian systems. In Broomhead, D. S. and Iserles, A., editors, *The Dynamics of numerics and the numerics of dynamics*, pages 137–193. Clarendon Press, Oxford.

Maeda, S. (1981). Lagrangian formulation of discrete systems and concept of difference space. *Math. Japonica*, 27(3):345–356.

Marsden, J. (1992). *London Mathematical Society Lecture Note Series 174: Lectures on Mechanics*. Cambridge University Press, Cambridge, England.

Marsden, J. and G. Patrick, G. (1996). *Integration Algorithms for Mechanical Systems*, volume 10 of *Fields Institute Communications*. American Mathematical Society.

Marsden, J. and Ratiu, T. (1994). *Introduction to Mechanics and Symmetry*. Springer-Verlag, New York.

Marsden, J. and Scheurle, J. (1993). Lagrangian reduction and the double spherical pendulum. *Z.A.M.P*, 44(1):17–43.

McLachlan, R. and Scovel, C. (1995). Equivariant constrained symplectic integration. *Journal of Nonlinear Science*, 5:233–256.

McLachlan, R. I. and Scovel, C. (1996). A survey of open problems in symplectic inegration. *Fields Institute Communications*, 10:151–180.

Moser, J. and Veselov, A. P. (1991). Discrete versions of some classical integrable systems and factorization of matrix polynomials. *Comm. in Mathematical Physics*, 139(2):217–243.

Murray, R., Li, Z., and Sastry, S. (1994). *A Mathematical Introduction to Robotic Manipulation.* CRC Press, Boca Raton, Fl.

Ortiz, M. (1986). A note on energy conservation and stability of nonlinear time-stepping algorithms. *Computers and Structures*, 24(1):167–168.

Reich, S. (1993). Symplectic integration of constrained hamiltonian systems by runge-kutta methods. Technical Report 93-13, University of British Columbia.

Reich, S. (1994). Momentum preserving symplectic integrators. *Physica D*, 76(4):375–383.

Ryckaert, J., Ciccotti, G., and Berendsen, H. (1977). Numerical integration of the cartesian equations of motion of a system with constraints: molecular dynamics of n-alkanes. *Journal of Computational Physics*, 23:327–341.

Sanz-Serna, J. (1991). Symplectic integrators for hamiltonian problems: an overview. *Acta Numerica*, 1:243–286.

Sanz-Serna, J. and Calvo, M. (1994). *Numerical Hamiltonian Problems.* Chapman and Hall, London.

Shibberu, Y. (1994). Time-discretization of hamiltonian systems. *Computers Math. Applic.*, 28(10-12):123–145.

Simo, J. and Gonzalez, O. (1993). Assessment of energy-momentum and symplectic schemes for stiff dynamical systems. In *ASME Winter Annual Meeting*, New Orleans. Nov. 28 - Dec. 3, 1993.

Simo, J. and Wong, K. (1991). Unconditionally stable algorithms for rigid body dynamics that exactly preserve energy and momentum. *International Journal for Numerical Methods in Engineering*, 31:19–52. Also see addendum, 33:1321-1323, 1992.

Simo, J. C. and Tarnow, N. (1992). The discrete energy-momentum method. conserving algorithms for nonlinear elastodynamics. *ZAMP*, 43:757–792.

Verlet, L. (1967). Computer experiments on classical fluids. *Phys. Rev*, 159:98–103.

Veselov, A. P. (1988). Integrable discrete-time systems and difference operators. *Funkts. Anal. Prilozhen.*, 22(2):1–13.

Veselov, A. P. (1991). Integrable lagrangian correspndences and the factorization of matrix polynomials. *Funkts. Anal. Prilozhen.*, 25(2):38–49.

Wendlandt, J. (1995). Pattern evocation and energy-momentum integration of the double spherical pendulum. MA thesis, University of California at Berkeley. Department of Mathematics, CPAM-656.

Wendlandt, J. and Sastry, S. (1996). Recursive workspace control of multibody systems: A planar biped example. In *IEEE Control and Decision Conference*, Kobe, Japan. Dec. 11-13, 1996.

Wisdom, J. and Holman, M. (1991). Symplectic maps for the n body problem. *Astronomical Journal*, 102(4):1528–1538.

Wolfram, S. (1991). *Mathematica: A System for Doing Mathematics by Computer.* Addison-Wesley, Red-Wood City, second edition.

Yoshida, H. (1990). Construction of higher order symplectic integrators. *Phys. Lett. A*, 150:262–268.